CHALMERS
UNIVERSITY OF TECHNOLOGY

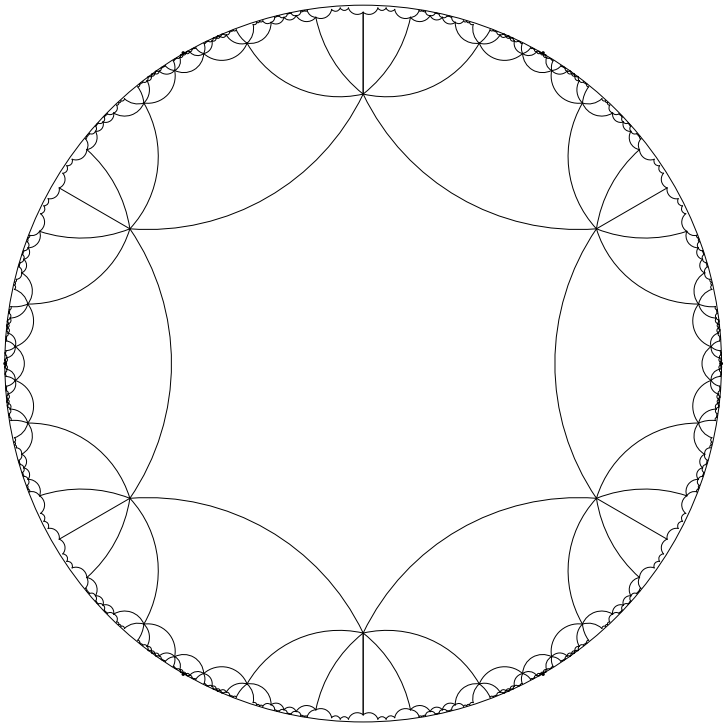

Holographic Plasmons in Graphene

Gauge/Gravity-duality as a Means to Describe Strongly Coupled Collective Excitations in Strange Metals

Master's thesis in Physics and Astronomy

MARCUS ARONSSON

Department of Physics
Chalmers University of Technology
Gothenburg, Sweden 2016

Master's thesis 2016

Holographic Plasmons in Graphene

Gauge/Gravity-duality as a Means to Describe Strongly Coupled Collective Excitations in Strange Metals

MARCUS ARONSSON

CHALMERS
UNIVERSITY OF TECHNOLOGY

Department of Physics
Division of Theoretical Physics
Chalmers University of Technology
Gothenburg, Sweden 2016

Holographic Plasmons in Graphene
Gauge/Gravity-duality as a Means to Describe Strongly Coupled Collective Excitations in Strange Metals
MARCUS ARONSSON

Supervisor: Ulf Gran, Department of Physics
Examiner: Ulf Gran, Department of Physics

Master's Thesis 2016
Department of Physics
Division of Theoretical Physics
Chalmers University of Technology
SE-412 96 Gothenburg
Telephone +46 31 772 1000

Cover: Regular hexagons in the Poincaré disk, a 2-dimensional space with negative curvature like AdS.
Figure generated through the Wolfram Demonstrations Project:
Tiling the Hyperbolic Plane with Regular Polygons
by Gašper Zadnik, published March 4, 2013.

Typeset in LaTeX
Printed by Chalmers Reproservice
Gothenburg, Sweden 2016

Holographic Plasmons in Graphene
Gauge/Gravity-duality as a Means to Describe Strongly Coupled Collective Excitations in Strange Metals
MARCUS ARONSSON
Department of Physics
Chalmers University of Technology

Abstract

Since its discovery in 2004, graphene has been a hot topic in research. As it is a two-dimensional material it has many exciting and often extreme properties. It has recently been shown to possess strongly coupled properties, implying that standard methods such as perturbation theory fails to properly depict the behaviour of graphene in certain regimes. One way to get around this is using the AdS/CFT-duality discovered by Maldacena in 1997. This approach has previously been carried out with success, predicting several properties of similar materials. One property that has yet to be described by such models however is the existence of plasmons.

The purpose of this thesis was therefore to investigate this issue. We built a top-down D3-D7'-model in the same fashion as previously done by Jokela et al. The model was then incorporated into Wolfram Mathematica for the numerical calculations. In the model we had a number of different choices that were either model specific (e.g. embeddings, stabilizing magnetic fluxes, boundary conditions) or physical quantities (e.g. temperature, charge density) that allowed for searches in a large parameter space. This flexibility allowed us to compare the results from our model with similar studies. However, no plasmons were found within the model. We discuss some possible shortcomings of the model and outline future research directions.

Keywords: gauge/gravity duality, holography, string theory, graphene, plasmons.

Acknowledgements

I would like to thank my supervisor Ulf Gran, without whom this project would not have been possible. I would also like to thank Tobias Wenger for many insightful discussions. My thanks to the division of Theoretical physics for taking me on, and helping me along the way. Lastly, for their persistent support, I thank my family and my friends.

Marcus Aronsson, Gothenburg, September 2016

Contents

1 Introduction **1**
- 1.1 Motivation . . . 1
- 1.2 Aim . . . 1
- 1.3 Objectives . . . 1
- 1.4 Scope . . . 2
- 1.5 Method . . . 2

2 Background **3**
- 2.1 Graphene . . . 3
- 2.2 AdS/CFT . . . 4
- 2.3 Plasmons . . . 4

3 Method and Theoretical Framework **7**
- 3.1 The Metric . . . 7
- 3.2 The D3/Dq-brane setup . . . 8
- 3.3 The Action . . . 11
- 3.4 Equations of motion . . . 14
- 3.5 Perturbations . . . 16
- 3.6 Boundary conditions . . . 19
  - 3.6.1 Background fields . . . 19
  - 3.6.2 Perturbation fields . . . 20

4 Model overview **23**
- 4.1 Mathematica: Initialization . . . 23
- 4.2 Mathematica: Large r asymptote . . . 24
- 4.3 Mathematica: Horizon limit . . . 24
- 4.4 Mathematica: Solver . . . 25
- 4.5 Validation . . . 25

5 Results **27**
5.1 Individual parameter impacts 27
5.1.1 d 28
5.1.2 ψ_0 28
5.1.3 Δ 29
5.1.4 Boundary conditions 30

6 Discussion and Conclusions **33**
6.1 Reliability of the model 33
6.2 The plasmon mode 33
6.2.1 Parameter space 33
6.2.2 Model improvements 34
6.3 Outlook 34

References **36**

Chapter 1

Introduction

1.1 Motivation

Graphene is a new and not very well studied material compared to many others. However it holds an immense potential with its unique properties in many different applications, making it the subject for intensive studies at many institutions around the world. It has also recently been observed that the electron-electron interaction in graphene is strongly coupled in a certain regime of parameter space, which is making it difficult, if not straight up impossible, to properly describe graphene theoretically with traditional means. Thanks to its many exciting properties, a model properly describing these strongly coupled tendencies is desired. One method that can be used to describe strongly coupled electromagnetic systems is the AdS/CFT-correspondence, which is a duality between a gravitational theory in anti-de Sitter-space and a conformal field theory on the boundary of that spacetime. This has been done to model graphene previously, however, to our knowledge, no plasmons have been modeled.

1.2 Aim

In this project, we aim to investigate a holographic model to describe graphene in a strongly coupled regime.

1.3 Objectives

There are several objectives we wish to achieve:

- We wish to build a Mathematica model that describes a holographic dual of a two dimensional material and lets the user compute relevant quantities.

- We wish to map which free parameters such a system has, for instance investigate which of them that can be fixed and which that are truly degrees of freedom.
- We wish to make the model customizable as to impose conditions on the material which can be translated into the dual, such as specifying charge densities, magnetic and electric fields.
- We wish to replicate results from other studies: Both theoretical studies of similar duality models but also experimental results, in particular the plasmon dispersion.

1.4 Scope

The project has many possible branches to work along once the model is constructed. Our main restrictions have been

- to work with a D3/D7' probe brane model,
- to have no dependencies on internal spheres
- and to have no external fields (although keep them possible for further studies).

1.5 Method

Firstly we did a literature study, identifying two fairly recent books, [1, 2], as an excellent starting point. Thereafter the D3/D7' probe brane model proposed by Jokela et al. in [3] was used. We have kept the system general and extended it along the directions of allowing fluctuations, and allowing anyonic boundary conditions. For near horizon boundary conditions we have used Frobenius expansions to solve the regular singular differential equations. For the far horizon boundary conditions the natural determinant method suggested in [4] was used.

Chapter 2

Background

This work is focused on the intersection of three individually promising areas of research; graphene, the AdS/CFT correspondence and plasmons.

2.1 Graphene

Graphene is a rather new and not very well studied material, but with immense potential. It consists of a single atomic layer of carbon, structured into a regular hexagonal grid. Theoretical descriptions of graphene have been done several decades ago, as a consideration of mono-layer graphite [5]. It was however considered a theoretical construction only, not practically obtainable. Novoselov and Geim managed to isolate these previously deemed impossible mono-layers of graphite in 2004 [6], and were awarded the Nobel Prize in Physics 2010 for this and the subsequent studies of graphene [7]. Several other perfectly two-dimensional materials have since then been produced and studied. Being two-dimensional gives these materials several exciting and often extreme properties. In addition to this, graphene has no band gap and a linear dispersion at the Dirac points, which makes it even more special. It is immensely strong and well conducting, but it also displays several more exotic properties such as an unusual quantum Hall effect and special types of tunneling [7]. Great scientific effort is put into graphene research, most notably the "Graphene Flagship" launched by the European Commission to take graphene out from academic laboratories and into society over the next decade.

Graphene has however been observed to behave strongly coupled in certain regimes. It being strongly coupled is in itself nothing uncommon; most metals have a coupling constant > 1, but they can often be described properly with Fermi-Landau theory as Fermi-liquids, a continuation of the weakly coupled electron gas. This circumstance is in some sense fortunate; that although the coupling

constant is large, turning up the coupling constant from small values passes no poles, no phase transition occurs and similar behaviour is expected [8]. This fortunate circumstance is not the case with graphene near the tip of the energy cone, where the Fermi surface effectively disappears and the screening is ineffective. This is why we say that the material behaves strongly coupled (and is often what one means when just saying that a material is strongly coupled) [9]. This means that the most common mathematical methods to study and model it, such as perturbation theory, falls short. There are very few other ways to study strongly coupled matter, but one promising candidate is the AdS/CFT correspondence.

2.2 AdS/CFT

The AdS/CFT correspondence is a powerful duality which was discovered by Maldacena in 1997 [10]. It is a duality between a string theory and a quantum field theory (or rather a conformal field theory). It allows one to describe an SU(N) gauge theory instead with a string theory in anti-de Sitter space. There are a few different limits that can be taken on the parameters on either side of the duality. The most common one takes the limit of $N >> 1$ and the coupling in the field theory to be strong. In this case, the string theory is still weakly coupled, which means that the strongly coupled field theory, in which most standard methods fail, can be accurately described by a weakly coupled theory. This is part of a larger statement, the *holographic principle*, which states that gravitational theories can aptly be described by their boundary. To have a four-dimensional field theory be described by the boundary of a ten-dimensional string theory, one introduces spherical coordinates for the remaining six coordinates. The boundary then means $r \to \infty$, and one is left with four-dimensional spacetime times a compact manifold, which can be reduced.

Several strongly coupled systems have been previously described using this gauge/gravity duality, most notably superconducting systems. It has also been used with success to describe strongly coupled two dimensional materials, describing several exotic phenomena such as the fractional quantum Hall effect [3] and roton states [11], as well as predicting more common properties such as conductivity. One thing that (to our knowledge) has yet to be described using this duality is the existence of plasmonic states.

2.3 Plasmons

Plasmons are collective excitations in a plasma, typically excited by incident light, hybridizing photons with electrons, producing almost sound-like waves, before

these decay and once again emit the bound light. The visible effects of such have been used for centuries, for instance using small metal grains to get the colours in stained glass [12]. It is however only during the last century in which they have been properly studied and understood, thanks to the development of electromagnetic theory. There are several different kinds of plasmons; transverse and longitudinal waves as well as bulk or surface bound plasmons. Thanks to their ability to have a shorter wave length than the incident light, there is hope to build very small optical devices, as the size of such are determined by the free wave length [13].

How to construct desirable plasmonic systems is of course a big question, and one of the leading candidates as a material to work with is graphene. Plasmons in graphene stands out from many different materials for several reasons, among these are the exceptionally low losses and large wave localization compared to other materials considered [13].

In this thesis we will focus mainly on longitudinal surface plasmons. These are very reminiscent of sound waves, but with charged particles transmitting the wave. They are also the charged version of zero sound modes, which are basically the wave modes at zero temperature for bosonic systems [14].

Chapter 3

Method and Theoretical Framework

The AdS/CFT correspondence is an explicit realisation of the *holographic principle*. The holographic principle states that in a general gravitational theory, in this case a string theory, the information contained in a bulk volume is described by information on its boundary [1].

In this project a very specific setup of the AdS/CFT correspondence was used. We consider a strongly coupled $\mathcal{N} = 4$ Super Yang-Mills SU(N)-theory in $3 + 1$ dimensions which is dual to a type IIB string theory in anti-de Sitter space, $AdS_5 \times S_5$. In the field theory we have a coupling strength g_{YM} and the SU(N)-group number N, and in the string theory we have a string length $l_s = \sqrt{\alpha'}$ and a coupling constant g_s. These are related to each other as

$$g_{YM}^2 = 2\pi g_s, \tag{3.1}$$

$$2g_{YM}^2 N = L^4/\alpha'^2, \tag{3.2}$$

where L is the AdS radius of curvature (that is, the cosmological constant part of the gravitational action is $\frac{1}{16\pi G}\frac{d(d-1)}{L^2}$ in $(d+1)$-dimensional space time) [1].

This is the general form, but typically one works in a limit of these parameters. We will be working in the limit

$$g_{YM}^2 \to 0, \tag{3.3}$$

$$g_{YM}^2 N \to \infty. \tag{3.4}$$

3.1 The Metric

This system is rather well studied from before that can shortly be argued for. An SU(N)-theory is roughly a U(N)-theory, which is what we get from a stack of N

coincident D-branes, on which the strings may have their endpoints. With our EM field theory living in 3+1 dimensions, so must the D-branes, that is we have D3-branes. Respecting the symmetries we get the following metric

$$\mathrm{d}s^2 = H(r)^{-1/2}\eta_{\mu\nu}\mathrm{d}x^\mu \mathrm{d}x^\nu + H(r)^{1/2}\delta_{ij}\mathrm{d}x^i\mathrm{d}x^j, \tag{3.5}$$

where $H(r) = 1 + L^4/r^4$ and μ,ν = 0,1,2,3, i,j = 4,...,9 [1]. We are working in what is known as the near horizon limit, $r \ll L$, in which case the metric simplifies. Let the stack of D3-branes denote the origin for the remaining 6 dimensions. These can be further decomposed into a distance from the D3-branes, r, and 5 angular coordinates, Ω_5. With the stack of D3-branes being a gravitational source, the metric becomes

$$\mathrm{d}s^2 = \frac{r^2}{L^2}\left(-h(r)\mathrm{d}t^2 + \mathrm{d}x^2 + \mathrm{d}y^2 + \mathrm{d}z^2\right) + \frac{L^2}{r^2 h(r)}\mathrm{d}r^2 + L^2\mathrm{d}\Omega_5^2, \tag{3.6}$$

where $h(r)$ is the emblackening factor $(1 - \frac{r_T^4}{r^4})$. Note that this is AdS for all values of r, where (3.5) would flatten for large r.

We rescale with L to work in dimensionless coordinates,

$$t \to Lt, \tag{3.7}$$
$$x \to Lx, \tag{3.8}$$
$$y \to Ly, \tag{3.9}$$
$$z \to Lz, \tag{3.10}$$
$$r \to Lr, \tag{3.11}$$

and end up with the rather standard black hole (brane) metric in AdS-space

$$L^{-2}\mathrm{d}s^2 = r^2\left(-h(r)\mathrm{d}t^2 + \mathrm{d}x^2 + \mathrm{d}y^2 + \mathrm{d}z^2\right) + \frac{\mathrm{d}r^2}{r^2 h(r)} + \mathrm{d}\Omega_5^2. \tag{3.12}$$

The (dimensionless) horizon radius r_T can be related to temperature T as

$$T = \frac{r_T}{\pi L}. \tag{3.13}$$

This can be shown by performing a Wick rotation and observing the periodicity of the euclidean time coordinate at the horizon. The radius of curvature can be related to the coupling constants g_s and α' by (3.2).

3.2 The D3/Dq-brane setup

To realize charged fermions living in the desired plane describing graphene, we want to consider open strings from this stack of branes but confining them to end

on another stack of D-branes which shares the first two spatial directions, allowing the strings to move freely only in the desired plane. As this is a type IIB-string theory, only odd-numbered D-branes are stable, leaving only three candidates: D3-, D5- and D7-branes (a D1-brane could not possibly share both the x and y directions and a D9-brane must share the z-direction as it fills the entire space). The geometrically possible D-brane setups can be viewed in table 3.1, with our specific choice of labeling the coordinates.

Table 3.1: Geometrically possible D-brane setups.

	x^0	x^1	x^2	x^3	x^4	x^5	x^6	x^7	x^8	x^9
	t	x	y	z	r	θ	ϕ	α	β	ψ
$D3$	•	•	•	•						
$D3$	•	•	•		•					
$D5$	•	•	•		•	•	•			
$D7$	•	•	•		•	•	•	•	•	

Of these three, only D7-branes are of particular interest to us as another stack of D3-branes would result in a tachyonic ground state, and a stack of D5-branes would leave the system supersymmetric. We are thus left with a stack of D7-branes. This leaves only the Ramond sector containing a massless state which is good because we wish to have only fermions in the plane [15]..

An important remark; We let a stack of D3-branes govern the metric, and then we introduce another stack of D7-branes. This stack would in theory also affect the metric, but what is significant is the number of such branes. If the number of D7-branes is negligible compared to the number of the D3-branes, their impact on the metric should be negligible too. This is called a probe limit, which we will be working with, and the D7-branes are what is referred to as probe-branes.

Another note to be made is that the D3-D7-brane setup selected is not yet unique. There are many different ways to chose a compact subset of S_5, with the different choices having a more significant impact, depending on how much you let the system depend on these not physically obvious angles. The three most intuitive choices are letting the ψ-coordinate split the "extra" 6-dimensional space into 1+5, 2+4 or 3+3 dimensions, as in table 3.2, and weight the content of each. Note that we still want r to be the distance to the origin, so these must square to 1, but that the choices of coordinates on the S_n of course could be made in other ways.

Table 3.2: Some divisions of the last 6 (cartesian) coordinates angular parts by ψ.

S_4	$S_1 \times S_3$	$S_2 \times S_2$
$\cos\psi$	$\cos\psi\cos\theta$	$\cos\psi\cos\theta$
$\sin\psi\cos\theta$	$\cos\psi\sin\theta$	$\cos\psi\sin\theta\cos\phi$
$\sin\psi\sin\theta\cos\phi$	$\sin\psi\cos\phi$	$\cos\psi\sin\theta\sin\phi$
$\sin\psi\sin\theta\sin\phi\cos\alpha$	$\sin\psi\sin\phi\cos\alpha$	$\sin\psi\cos\alpha$
$\sin\psi\sin\theta\sin\phi\sin\alpha\cos\beta$	$\sin\psi\sin\phi\sin\alpha\cos\beta$	$\sin\psi\sin\alpha\cos\beta$
$\sin\psi\sin\theta\sin\phi\sin\alpha\sin\beta$	$\sin\psi\sin\phi\sin\alpha\sin\beta$	$\sin\psi\sin\alpha\sin\beta$

The last of these options was used, letting the four compact coordinates included in the D7-branes be $S_2 \times S_2$, in what has been called the D3-D7' setup (with D3-D7 implying the S_4 version).

Table 3.3: Domains for the angular coordinates for the D3/D7'-brane setup

$$\begin{aligned} \psi &\in [0,\pi/2] \\ \theta &\in [0,\pi] \\ \phi &\in [0,2\pi) \\ \alpha &\in [0,\pi] \\ \beta &\in [0,2\pi) \end{aligned}$$

Another aspect to be considered is the extension of our coordinates. Where spacetime is naturally expanded, we have the consideration of the remaining coordinates, primarily the radial coordinate r for the D7-branes, for which we have basically two different possibilities. Either there is a gap between the two stacks of branes, giving a finite, non-zero minimum string length, or there is none.

The first case means the brane needs to have a tip of some sort, located at $\psi = 0$ or $\psi = \pi/2$, and some $r = r_0$, which dictates the minimal distance between the two stacks of branes.

The second case, where there is no gap between the two stacks of branes, is what is called a black hole embedding. As the name suggests, at some point the D7-branes cross the black brane horizon $r = r_T$. The degree of freedom that was before the minimal string length now becomes the angle ψ where the D7-branes cross the horizon. An angle that is not $\psi = \psi_\infty$ would suggest a non-zero minimal string length within the horizon, which is arguably not quite non-zero, but still

less than the energy scale of the system. The different types of embeddings can be seen in figure 3.1.

As we wish to model graphene, which has a linear cone in its band structure with no gap, black hole-embeddings is the choice made, and most likely with an initial angle that is $\psi_0 = \psi_\infty$. In this report however, we will try to keep most calculations general.

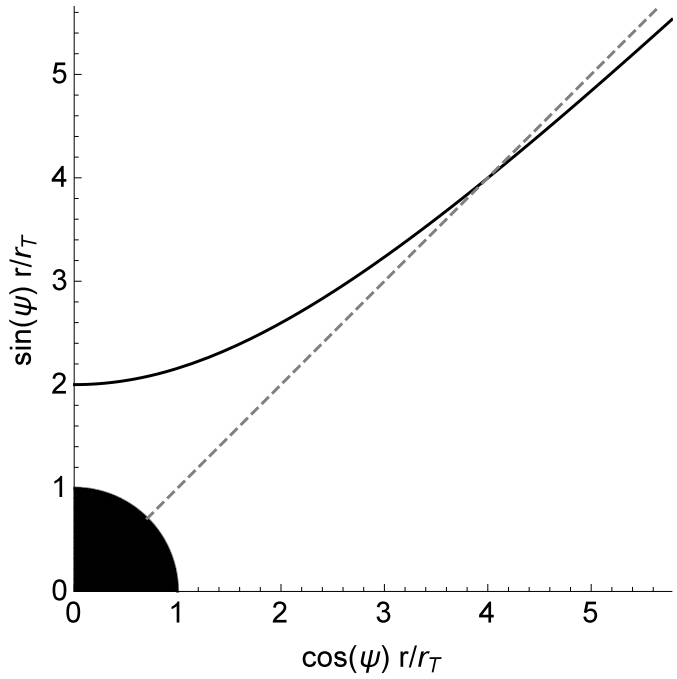

Figure 3.1: Different embeddings for the D7-branes. The black line corresponds to Minkowski-embeddings, where there is a non-zero minimal distance between the D7-branes and the D3-branes (located at the origin in the figure). The dashed, gray line corresponds to a black hole-embedding, where the D7-branes crosses the horizon induced by the D3-branes. The fundamental freedom for the different embeddings are the minimal distance between branes in the Minkowski-embedding (where the brane reaches the vertical axis) and for black hole-embeddings the angle at which the horizon is crossed.

3.3 The Action

D3-D3-strings and closed strings are part of the background theory and not interesting here. D7-D7-strings are negligible because of the probe approximation. Left

is only the action for the open strings between D3 and D7-branes. This means it suffices to consider a Dirac-Born-Infeld (DBI) action, with a Chern-Simons term (CS),

$$\int \mathcal{L} = \int \mathcal{L}_{DBI} + \int \mathcal{L}_{CS}. \tag{3.14}$$

where

$$\mathcal{L}_{DBI} = -T_7\sqrt{-\operatorname{Det}\left(g_{ij} + 2\pi\alpha' F_{ij}\right)}, \tag{3.15}$$

(i,j are indices on the D7-branes).

With the metric in (3.12) and letting the excluded coordinates depend on only r,

$$z = z(r), \tag{3.16}$$
$$\psi = \psi(r), \tag{3.17}$$

we get the induced metric on the D7-branes to be

$$\begin{aligned} L^{-2}\mathrm{d}s_7^2 =& r^2\left(-h(r)\mathrm{d}t^2 + \mathrm{d}x^2 + \mathrm{d}y^2\right) + \\ & \frac{1}{h(r)r^2}\left(1 + h(r)r^4\, z'(r)^2 + h(r)r^2\psi'(r)^2\right)\mathrm{d}r^2 + \\ & \sin\psi^2\left(\mathrm{d}\theta^2 + \sin^2\theta\,\mathrm{d}\phi^2\right) + \cos\psi^2\left(\mathrm{d}\alpha^2 + \sin^2\alpha\,\mathrm{d}\beta^2\right). \end{aligned} \tag{3.18}$$

The Chern-Simons term is a topological addition to the action [1]

$$\mathcal{L}_{CS} = -T_7\sum_q P[C_{(q+1)}]e^{2\pi\alpha' F}, \tag{3.19}$$

where the exponential should be seen as the corresponding series but in terms of the wedge product. It has two possible non-vanishing terms:

$$\mathcal{L}_{CS} = -T_7\frac{(2\pi\alpha')^2}{2}P[C_4]\wedge F\wedge F, \tag{3.20}$$

$$\mathcal{L}_{CS} = -T_7\frac{(2\pi\alpha')^4}{4!}P[C_0]F\wedge F\wedge F\wedge F, \tag{3.21}$$

where the 4-form in (3.20) comes from the D3-branes and the 0-form in (3.21) from the D7-branes. The latter is negligible for this reason (and arguably also because of the higher order of α'). The 4-form can be written as

$$C_4 = L^4 \left(r^4 \mathrm{d}t \wedge \mathrm{d}x \wedge \mathrm{d}y \wedge \mathrm{d}z - \frac{1}{2} c(\psi) \mathrm{d}\Omega_2^{(1)} \wedge \mathrm{d}\Omega_2^{(2)} \right). \tag{3.22}$$

A short derivation of this; Starting with the 4-form

$$L^4 r^4 \mathrm{d}t \wedge \mathrm{d}x \wedge \mathrm{d}y \wedge \mathrm{d}z, \tag{3.23}$$

we get the 5-form $\mathrm{d}C_4$ to be

$$4L^4 r^3 \mathrm{d}t \wedge \mathrm{d}x \wedge \mathrm{d}y \wedge \mathrm{d}z \wedge \mathrm{d}r. \tag{3.24}$$

This should be self dual, so the $S_2 \times S_2$ contribution to the 5-form must be

$$-4L^4 \sin\alpha \sin\theta \sin^2\psi \cos^2\psi \, \mathrm{d}\psi \wedge \mathrm{d}\theta \wedge \mathrm{d}\phi \wedge \mathrm{d}\alpha \wedge \mathrm{d}\beta = -4L^4 \, \mathrm{d}\Omega_5. \tag{3.25}$$

Integrating back this expression yields

$$-\frac{1}{2}\left(\psi - \frac{1}{4}\sin 4\psi + const\right) L^4 \sin\theta \sin\alpha \mathrm{d}\theta \wedge \mathrm{d}\phi \wedge \mathrm{d}\alpha \wedge \mathrm{d}\beta = -\frac{1}{2} c(\psi) L^4 \mathrm{d}\Omega_2^{(1)} \wedge \mathrm{d}\Omega_2^{(2)}, \tag{3.26}$$

where we have defined $c(\psi) = \psi - \frac{1}{4}\sin 4\psi + const$. Setting this constant corresponds to adding a boundary term to the action, which does not change the bulk physics. Here we set it so that $c(\psi_\infty) = 0$.

The next step is to consider the field strength F_{ij}, where we firstly need to introduce fluxes through the S_2-spheres. This must be done to stabilize the setup, otherwise the different D-brane stacks would repel each other and the system would be unstable. This magnetic field needs no theoretical motivation, as it is rather a degree of freedom for any system. This is the same effect one gets when dissolving lower-dimensional D-branes in the D7-branes, which consequently quantifies the fluxes [16]. This is where the choice of angular coordinates really makes a difference. In our case, we get one flux through each S_2, and it is quite obvious that the other setups get different fluxes,

$$2\pi\alpha' F_{\theta\phi} = -\frac{L^2}{2}\sin\theta f_1, \tag{3.27}$$

$$2\pi\alpha' F_{\alpha\beta} = -\frac{L^2}{2}\sin\alpha f_2, \tag{3.28}$$

where the fluxes are quantized $f_i = \frac{2\pi\alpha'}{L^2} n_i$, with n_i some integers. It is worth noting that for the system to remain parity invariant, something that is of physical relevance for graphene, the spheres must be interchangeable, and thus the fluxes be equal [17].

We should also include a radial part of the gauge field, $a_r(\ldots)$, but our gauge choice is to keep this identically zero.

Lastly one must allow for a charge density in the bulk of the D7-branes, giving rise to

$$2\pi\alpha' F_{tr} = L^2 a_0'(r). \tag{3.29}$$

This is the base system, onto which we may add more fields to get other interesting systems.

The Lagrangians can now be written more concisely

$$\mathcal{L}_{DBI} = \mathcal{N}\int \mathrm{d}r\, \frac{r^2}{2}\sqrt{(f_1^2 + 4\cos^4\psi)\left(f_2^2 + 4\sin^4\psi\right)}\times \sqrt{1 - a_0'^2 + r^4 h(r) z'^2 + r^2 h(r)\psi'^2}, \tag{3.30}$$

$$\mathcal{L}_{CS} = \mathcal{N}\int \mathrm{d}r\, \frac{1}{2} f_1 f_2 r^4 z'(r), \tag{3.31}$$

where we have defined $\mathcal{N} = 8L^8\pi^2 T_7 V_{1,2}$ and $V_{1,2} = \int \mathrm{d}t\mathrm{d}x\mathrm{d}y$.

3.4 Equations of motion

To find the background equation of motions the action is varied with respect to z, a_0 and ψ yielding:

$$\partial_r\left(g(r) r^8 h(r) z' - \frac{1}{2} f_1 f_2 r^4\right) = 0, \tag{3.32}$$

$$\partial_r\left(g(r) r^4 a_0'\right) = 0, \tag{3.33}$$

and

$$\partial_r\left(g(r) r^6 h(r)\psi'\right) - \frac{2\sin\psi\cos\psi}{g(r)}\left(\sin^2\psi\left(f_1^2 + 4\cos^4\psi\right) - \cos^2\psi\left(f_2^2 + 4\sin^4\psi\right)\right) = 0, \tag{3.34}$$

where we have defined

$$g(r) = \frac{\sqrt{f_1^2 + 4\cos^4\psi}\sqrt{f_2^2 + 4\sin^4\psi}}{2r^2\sqrt{1 - a_0'^2 + r^4 h(r) z'(r)^2 + r^2 h(r)\psi'(r)^2}}. \tag{3.35}$$

The z and a_0 equations are fairly straightforward to solve as functions of ψ but the ψ equation itself is rather a mess to sort out. The first two equations can clearly be integrated once, giving a pair of integration constants in the process,

$$c_z = g(r)r^8 h(r)z' - \frac{1}{2}f_1 f_2 r^4, \tag{3.36}$$

$$d = g(r)r^4 a_0'. \tag{3.37}$$

The z equation's integration constant can be found, as only a specific value of it is consistent, depending on the embedding. The a_0 equation's integration constant however is truly a degree of freedom corresponding to that of a physical charge density. As only a_0' and z' show up in calculations, these derivatives may instead be considered the fields to find, rendering their corresponding equations of motion algebraic,

$$g = \frac{\sqrt{4r^4 h\left(d^2 + \frac{1}{4}r^4\left(f_2^2 + 4\sin^4\psi\right)\left(f_1^2 + 4\cos^4\psi\right)\right) - \left(f_1 f_2 r^4 + 2c_z\right)^2}}{2r^6\sqrt{h}\sqrt{r^2 h\psi'^2 + 1}}, \tag{3.38}$$

$$z' = \frac{\left(f_1 f_2 r^4 + 2c_z\right)\sqrt{r^2 h\psi'^2 + 1}}{r^2\sqrt{h}\sqrt{4r^4 h\left(d^2 + \frac{1}{4}r^4\left(f_2^2 + 4\sin^4\psi\right)\left(f_1^2 + 4\cos^4\psi\right)\right) - \left(f_1 f_2 r^4 + 2c_z\right)^2}}, \tag{3.39}$$

$$a_0' = -\frac{2r^2 d\sqrt{h}\sqrt{r^2 h\psi'^2 + 1}}{\sqrt{4r^4 h\left(d^2 + \frac{1}{4}r^4\left(f_2^2 + 4\sin^4\psi\right)\left(f_1^2 + 4\cos^4\psi\right)\right) - \left(f_1 f_2 r^4 + 2c_z\right)^2}}. \tag{3.40}$$

Some other physical quantities one might want are electric fields, magnetic fields and currents in the system, corresponding to the integration constants for the additional equations of motion one gets from adding those.

Expanding the ψ equation at $r = \infty$ lets one relate the magnetic fluxes to geometrical quantities instead. The dominating non-vanishing term lets us specify the end angle, as a function of f_1 and f_2. To keep them both real, the end angle is only allowed in an interval $0.2\pi \lesssim \psi_\infty \lesssim 0.3\pi$, with the extrema corresponding to one field being zero, and the mid-value corresponding to them being equal. This is shown in figure 3.2. The latter is specifically chosen, to keep the system parity invariant.

The next order of terms in the expansion lets us specify the fashion in which ψ approaches ψ_∞. In an expansion $\psi = \psi_\infty + mr^\Delta$, it lets us specify Δ. The equations to first order in m become

$$\Delta(\Delta + 3) = \frac{f_1^2 + 4\left(2\cos\left(2\psi_\infty\right) - 1\right)\cos^4\left(\psi_\infty\right)}{f_1^2 + 4\cos^6\left(\psi_\infty\right)}. \tag{3.41}$$

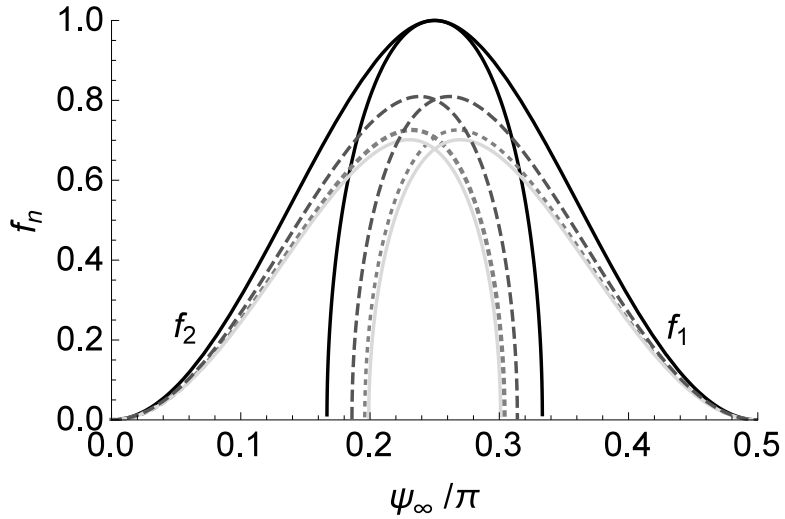

Figure 3.2: Values of the magnetic fluxes through the S_2's as functions of ψ. Curves from the left are the values of f_2, from the right are for f_1. From top to bottom (darkest to lightest) the curves correspond to $\Delta \to 0$, $\Delta = -1/2$, $\Delta = -1$ and $\Delta = -3/2$. If for a given Δ and ψ_∞ only one of the fluxes have a real value, the choice of asymptote is unstable. Note that only for $\psi_\infty = \pi/4$ is $f_1 = f_2$.

One sees that Δ can take values from 0 to $-3/2$ (0 or above makes no sense in an expansion, and below $-3/2$ is subleading, as the roots to (3.41) are symmetric around $-3/2$). The most noteworthy candidates are $\Delta = -1$ in which case the parameter m can actually be interpreted as a mass, and $\Delta = -1/2$ and $\Delta = -3/2$ as potential candidates to reflect the non-relativistic behaviour of a plasmon ($\omega \sim \sqrt{k}$).

3.5 Perturbations

Our interests lie mainly in the perturbations of this system, as that is where we would find (collective) excitations so now we introduce small fluctuations of the system. To keep these fluctuations consistent, one must include all possible types of fluctuations. This means perturbations need to be allowed in most fields and depend on many of the D7-brane coordinates. We follow the lines of [11]:

$$z \to z(r) + \epsilon\delta z(t,x,y,r), \tag{3.42}$$
$$\psi \to \psi(r) + \epsilon\delta\psi(t,x,y,r), \tag{3.43}$$
$$a_t \to a_0(r) + \epsilon\delta a_t(t,x,y,r), \tag{3.44}$$
$$a_x \to \epsilon\delta a_x(t,x,y,r), \tag{3.45}$$
$$a_y \to \epsilon\delta a_y(t,x,y,r), \tag{3.46}$$
$$a_r \to \epsilon\delta a_r(t,x,y,r), \tag{3.47}$$

where we have made the reasonable restriction to exclude dependencies on the four internal angular coordinates.

Inserting these into the action gives us

$$\mathcal{L} = \mathcal{L}^{(0)} + \epsilon\mathcal{L}^{(1)} + \epsilon^2\mathcal{L}^{(2)} + \dots. \tag{3.48}$$

The zero-order Lagrangian gives the background equations of motion. The first order Lagrangian is automatically zero by the solutions to the zero-order Lagrangian and the second order Lagrangian gives a set of equations of motions for the perturbations.

After the variation, wavelike conditions are imposed on the fluctuations. Due to rotational invariance in the xy-plane, we set the wave to be in the x-direction:

$$\begin{gathered}\delta z(t,x,y,r) \to \delta z(r) e^{-i\omega t + kx}, \\ \dots\end{gathered} \tag{3.49}$$

We also switch to the gauge invariant combination using $\delta e_x = k\delta a_t + \omega\delta a_x$. The reason for this is primarily that it is the more naturally occuring combination in expressions, which is of interest when we do various transformations. Our gauge choice is to keep $a_r = 0$, which we must also impose on the perturbations. This is of course done after the variations, which means there will be one more equation than the number of variables. This provides a check on the obtained equations, that one of the equations must be a linear combination of the others.

In the following equations, the dependence on r is omitted to save space. Any primes are derivatives with respect to r (derivatives on t only return a $-i\omega$, on x return a ik and on y nothing).

Varying the action with respect to δe_x yields

$$\begin{aligned}\partial_r\left(\frac{g}{\omega}r^4 h\left(\delta e_x' - k\delta a_t'\right)\right) = {} & gkr^4\omega a_0' z'\delta z + gkr^2\omega a_0'\psi'\delta\psi \\ & + i\omega\partial_r(c(\psi))\delta a_y - \frac{g\omega\left(hr^4 z'^2 + hr^2\psi'^2 + 1\right)}{h}\delta e_x,\end{aligned} \tag{3.50}$$

with respect to δa_y yields

$$\partial_r \left(gr^4 h \delta a_y'\right) = ika_0' \sin^2(2\psi)\delta\psi - g\left(\omega^2 \frac{(hr^4 z'^2 + hr^2\psi'^2 + 1)}{h} - k^2 A\right)\delta a_y - i\partial_r(c(\psi))\delta e_x, \quad (3.51)$$

with respect to δz yields

$$\begin{aligned}\partial_r \left(gh^2 r^{10} \frac{\psi' z'}{A}\delta\psi'\right) - \partial_r \left(ghr^8 \frac{a_0' z'}{A}\delta a_t'\right) \\ + \partial_r \left(ghr^8 \frac{(a_0'^2 - r^2 h\psi'^2 - 1)}{A}\delta z'\right) + \partial_r \left(gr^8 hBz'\delta\psi\right) \\ = \left(gk^2 r^4 \left(a_0'^2 - r^2 h\psi'^2 - 1\right) + \frac{gr^2\omega^2 \left(r^4 h\psi'^2 + r^2\right)}{h}\right)\delta z \\ - gkr^4 a_0' z'\delta e_x + gr^6 \left(k^2 h - \omega^2\right)\psi' z'\delta\psi, \quad (3.52)\end{aligned}$$

with respect to $\delta\psi$ yields

$$\begin{aligned}\partial_r \left(gr^6 hB\psi'\delta\psi\right) + \partial_r \left(gr^{10} h^2 \frac{z'\psi'}{A}\delta z'\right) \\ - \partial_r \left(gr^6 h \frac{\psi' a_0'}{A}\delta a_t'\right) - \partial_r \left(gr^6 h \frac{(hz'^2 r^4 - a_0'^2 + 1)}{A}\delta\psi'\right) = \\ + hgr^8 Bz'\delta z' + hgr^6 B\psi'\delta\psi' + gr^6 \left(k^2 h - \omega^2\right) z'\psi'\delta z + gr^4 Ba_0'\delta a_t' \\ + gr^4 CA\delta\psi \\ gr^2 \left(\omega^2 \left(z'^2 r^4 + \frac{1}{h}\right) - k^2 \left(hz'^2 r^4 - a_0'^2 + 1\right)\right)\delta\psi \\ - gk\psi' a_0' r^2 \delta e_x + 2ik \sin^2(2\psi) a_0' \delta a_y, \quad (3.53)\end{aligned}$$

with respect to δa_t yields

$$\begin{aligned}\partial_r \left(gr^4 Ba_0'\delta\psi\right) + \partial_r \left(ghr^8 \frac{a_0' z'}{A}\delta z'\right) + \partial_r \left(ghr^6 \frac{a_0'\psi'}{A}\delta\psi'\right) \\ - \partial_r \left(gr^4 \frac{hr^4 z'^2 + hr^2\psi'^2 + 1}{A}\delta a_t'\right) - ik\partial_r(c(\psi)\delta a_y) \\ = gk^2 r^4 a_0' z'\delta z + gk^2 r^2 a_0'\psi'\delta\psi - ikc(\psi)\delta a_y' \\ - gk\left(\frac{1}{h} + r^4 z'^2 + r^2\psi'^2\right)\delta e_x, \quad (3.54)\end{aligned}$$

and a final constraint from varying with respect to δa_r,

$$0 = \omega g r^4 B a_0' \delta\psi + g r^8 \frac{\omega h a_0'}{A} z' \delta z' + g r^6 \frac{\omega h a_0'}{A} \psi' \delta\psi' \\ - g r^4 \omega \frac{h r^4 z'^2 + h r^2 \psi'^2 + 1}{A} \delta a_t' - g h r^4 \frac{k}{\omega} \left(\delta e_x' - k \delta a_t' \right). \quad (3.55)$$

Here we have defined

$$A = h \left(r^2 z'^2 + \psi'^2 \right) r^2 - {a_0'}^2 + 1, \quad (3.56)$$

$$B = \left(\frac{8 \sin\psi \cos^3\psi}{f_1^2 + 4\cos^4\psi} - \frac{8 \sin^3\psi \cos\psi}{f_2^2 + 4\sin^4\psi} \right), \quad (3.57)$$

and

$$C = \left(\left(\frac{8 \cos\psi \sin^3\psi}{4\sin^4\psi + f_2^2} + \frac{8\cos^3\psi \sin\psi}{4\cos^4\psi + f_1^2} \right)^2 \right. \\ \left. - \frac{8\left(1 + 2\cos(2\psi)\right)\sin^2\psi}{4\sin^4\psi + f_2^2} - \frac{8\left(1 - 2\cos(2\psi)\right)\cos^2\psi}{4\cos^4\psi + f_1^2} \right). \quad (3.58)$$

Imposing the constraint on the other equations lets us eliminate δa_t, and also gives that the δa_t equation of motion is a linear combination of the others, leaving us with four coupled, linear, second-order differential equations and four fields.

3.6 Boundary conditions

3.6.1 Background fields

For Minkowski embeddings, the tip needs to be smooth, which sets a condition on the derivatives at this point. In a formulation with r and ψ, this condition turns into $\psi'(r) \to \infty$ as $r \to r_0$, implying that the brane expansion is set by a single parameter, the minimal distance r_0.

For black hole embeddings the ψ equation of motion is singular at the horizon. Making an expansion at the horizon reveals that the second derivative disappears at the horizon, and the system is fully defined by the ψ angle at which the brane crosses the horizon. That is, although it is a second order differential equation, we only get one degree of freedom, just as in the Minkowski case.

Regularity conditions sets the value of the z-equation of motion integration constant.

In Minkowski embeddings, regularity of the metric at $r = r_0$ enforces

$$c_z = -\frac{1}{2} f_1 f_2 r_0^4, \tag{3.59}$$

as the rr-part of the metric at that point, using $\mathrm{d}r = (\psi')^{-1}\mathrm{d}\psi$, is

$$\frac{1}{h(r_0)r_0^2}\frac{1 + h(r_0)r_0^4 z'(r_0)^2 + h(r_0)r_0^2\psi'(r_0)^2}{\psi'(r_0)^2}\mathrm{d}\psi^2 \tag{3.60}$$

and thus $z'(r_0)$ can not be more singular than $\psi'(r_0)$.

In black hole embeddings, consistency of the of the z-equation of motion (3.39) demands

$$c_z = -\frac{1}{2} f_1 f_2 r_T^4, \tag{3.61}$$

or else $z' \sim (r - r_T)^{-1/2}$ as for r close to r_T.

3.6.2 Perturbation fields

The boundary conditions imposed on the perturbation fields depend on the choice of embedding used. For Minkowski embeddings, we require that the tip is smooth, meaning that the derivatives of all fields have to be zero. This eliminates half of the boundary conditions and we have four degrees of freedom left out of the eight we started with.

For black hole embeddings the equations become regular singular at the horizon. A Frobenius expansion at the horizon lets us bypass this problem, as well as split the 8 degrees of freedom into two groups: In-falling solutions and out-going ones. By requiring in-falling solutions, any linear combination of those four are a solution, and we are once again left with four degrees of freedom.

A Frobenius expansion is classically only done in one variable, but the extension to multivariable systems is quite intuitive. At it's core, what one does is to replace a field by an expansion

$$q(r) = (r - r_0)^\gamma \left(\alpha_0 + (r - r_0)\alpha_1 + (r - r_0)^2\alpha_2 + \ldots\right), \tag{3.62}$$

which for a system where the coefficient in front of the second derivative has a zero of multiplicity 2 at r_0 and the coefficient in front of the first derivative has a zero of multiplicity 1 at r_0 naturally has two different solutions based on γ, with them being the solutions to a quadratic equation. This implies that we get complex exponents where we can identify one as in-falling and one as out-going. Clearly each of these solutions are scalable by a numerical factor, so for uniqueness, one sets $\alpha_0 = 1$. The multivariate expansion is nothing but expanding

the other fields in the same fashion, but keeping the same exponent as the infalling behaviour should be the same. As the solutions are scalable we can set the zero order coefficient of *one* of the expansions to be unity. A good check to verify the obtained solutions is that one gets 8 distinct solutions, paired up, and with dependencies on all different zero-orders (implying we have the maximum number of solutions in a linear system).

The remaining degrees of freedom are fixed by a condition at $r \to \infty$. The common requirement is that the perturbations should go to zero (Dirichlet boundary conditions), but there are other possibilities, such as Neumann boundary conditions or more generic Robin conditions. These are alternative quantizations of particles (bosonic, anyonic rather than fermionic) [18].

As the system is linear, a convenient method of obtaining the solution is the following determinant method as suggested by Amado et al [4]. Suppose that there is a solution with the desired boundary conditions. Then it can be written as a linear combination of the individual solutions we acquired from the Frobenius expansion,

$$\text{sol} = c_1\text{sol}_1 + c_2\text{sol}_2 + c_3\text{sol}_3 + c_4\text{sol}_4. \tag{3.63}$$

Writing the boundary values as a system of linear equations

$$\begin{aligned}
\delta z|_{r\to\infty} &= c_1\delta z_1 + c_2\delta z_2 + c_3\delta z_3 + c_4\delta z_4|_{r\to\infty},\\
\delta e_x|_{r\to\infty} &= c_1\delta e_{x1} + c_2\delta e_{x2} + c_3\delta e_{x3} + c_4\delta e_{x4}|_{r\to\infty},\\
\delta a_y|_{r\to\infty} &= c_1\delta a_{y1} + c_2\delta a_{y2} + c_3\delta a_{y3} + c_4\delta a_{y4}|_{r\to\infty},\\
\delta \psi|_{r\to\infty} &= c_1\delta \psi_1 + c_2\delta \psi_2 + c_3\delta \psi_3 + c_4\delta \psi_4|_{r\to\infty},
\end{aligned}$$

we can identify a matrix equation,

$$\begin{bmatrix} \delta z \\ \delta e_x \\ \delta a_y \\ \delta \psi \end{bmatrix}|_{r\to\infty} = \underbrace{\begin{bmatrix} \delta z_1 & \delta z_2 & \delta z_3 & \delta z_4 \\ \delta e_{x1} & \delta e_{x2} & \delta e_{x3} & \delta e_{x4} \\ \delta a_{y1} & \delta a_{y2} & \delta a_{y3} & \delta a_{y4} \\ \delta \psi_1 & \delta \psi_2 & \delta \psi_3 & \delta \psi_4 \end{bmatrix}}_{M} \times \begin{bmatrix} c_1 \\ c_2 \\ c_3 \\ c_4 \end{bmatrix}|_{r\to\infty}. \tag{3.64}$$

This system only has a non-trivial solution if Det $M = 0$. That is, we evaluate the determinant of this matrix (or the corresponding one for the choice of boundary condition at infinity) for different values of k and ω. For each value of k, a range of values for ω are tried, and from the resulting values of the determinant, solutions are extracted where those are zero.

The differential equations decouples for certain parameter values, such as $\psi' = 0$ and $d = 0$. This can be used to inspect the observed dispersion relations' origin.

Tracing a curve to this decoupling limit allows one to see which particular fields become linearly dependent. As we are interested in longitudinal modes mainly, we wish to study what comes from δe_x rather than δa_y.

Chapter 4

Model overview

The model was realized in Wolfram Mathematica. Symbolic derivations of the equations were made as to confirm the results obtained by pen and paper and numeric calculations were carried out to obtain the final results.

The model was split in several pieces as suitable.

4.1 Mathematica: Initialization

The program begins with an initial part that sets the metric and applied fields and produces the explicit form of the action. Variation then gives the equations of motion.

Main restrictions from a general model that are made here are

- $S_2 \times S_2$ geometry of the D7-branes.
- Only a charge density in the gauge fields (no external magnetic fields, electric fields or currents).
- The signs on the Chern-Simons term.

A special note to be made is the choice of signs for the Chern-Simons term and the four-form. Some literature differ in regards to what signs those should be, but we have chosen to have the space-time part positive and the angular part negative. This appears to have a rather negligible effect on the results and it can be argued that this should be the case (little change between branes/anti-branes, dual/anti-dual).

4.2 Mathematica: Large r asymptote

The second part treated the zero order fields at $r \to \infty$ as to let us control the system by adjusting the asymptotic behaviour, rewriting f_1 and f_2 as functions of ψ_∞ and Δ in the expansion $\psi = \psi_\infty + mr^\Delta$ for large r.

Main restrictions from a general model that are made here are

- Parity invariance ($f_1 = f_2$, equivalent to setting $\psi_\infty = \pi/4$).
- Asymptotic exponent, $\Delta = -1/2, -1, -3/2$.

This completely fixes f_1 and f_2.

4.3 Mathematica: Horizon limit

The third part treated the near horizon part. Here we made an ordinary Taylor expansion for the ψ field as the numerical solver of Mathematica struggles with the disappearing second order derivative. This expansion is only used in a very small part, until we solve for a generic ψ in the majority of the r-domain. Similarly, the perturbation fields were treated with a multivariate Frobenius expansion to fifth order.

Main restrictions from a general model that are made here are

- Black hole embeddings.
- Initial starting condition, $\psi_0 = \pi/4$,$1.1\pi/4$.
- Temperature radius, $r_T = 0.01$, 0.1, 1, 10[1].
- Charge density, $d =$ 0,1,10,1000.
- Numerical offset from the horizon, $\Delta r = 0.001$.
- Numerical infinity, $R_\infty = 10^5$.

The ψ equation was here solved with Mathematica's `NDSolve` routine. The solution, along with the Frobenius expansions, were passed on to the last part.

[1]The effect of changing the temperature radius will be discussed in the next section

4.4 Mathematica: Solver

The last part solved the equations of motion by supplying the final two unknown quantities, ω and k. The equations of motion were solved with the different initial conditions supplied by the Frobenius expansion. The solutions where then taken to the numerical infinity, where the determinant was computed as proposed in the theory section.

Main restrictions from a general model that are made here are

- Boundary end-conditions ($\delta\psi = \delta z = 0$, $\delta e_x' = \delta a_y' = 0$) and ($\delta\psi = \delta z = \delta e_x = \delta a_y = 0$)

For each pair of (ω,k) the determinant was computed. Sweeping over a range of different ω's for a fixed k, yields a complex curve. Where this curve has zeroes, the total boundary conditions has a non-trivial solution, and there exists particle states. Doing this, for a range of different k's yields a dispersion relation for those particle states.

It is important to note that the ω's can be complex, implying decaying modes, which is the expected behaviour for collective excitations at non-zero temperature.

4.5 Validation

Apart from examining possible plasmon modes in the model, we also made sure the model could reproduce the results from similar projects (for instance [19]). This was done both for the equations obtained, as well as the dispersion relations coming from the numerical calculations.

Chapter 5

Results

Despite extensive searches in the possible parameter space, we did *not* find any plasmons. This includes both the $\omega \sim \sqrt{k}$ behaviour predicted by Hwang et al. [20] for zero temperatures, or a massive plasmon mode, see for instance Godfrin et al. [14]

This includes alternating the signs of the 4-form, alternating between Dirichlet and Neumann boundary conditions for the gauge fields, zero and a non-zero mass, zero and non-zero charge density, the asymptotic exponent Δ and non-zero temperatures. The four latter were tried out for a range of different values. It should however be noted that one can rescale the frequency, wave vector and fields to make the equations of motion independent of the temperature, as is done by Jokela et al[19]. This implies that the model is not dependent on temperature and charge density individually, but rather on the ratio between them (for the existence of excitation modes that is).

We did find a zero-sound mode, with either Neumann or Dirichlet conditions. The Dirichlet conditions have a decaying zero-sound mode, as was shown in [19], whereas the zero-sound mode for Neumann conditions was stable. The latter is aThese results are shown in figure 5.1. For Dirichlet conditions, we see an initial purely dissipative mode for very small values of k. We also found another completely dissipative mode which originates from the transverse part δa_y, but as we are interested in longitudinal modes, we did not investigate this mode further.

5.1 Individual parameter impacts

As there are relatively many different parameters that were adjusted, here follows a brief summary of the impact of these individual parameters.

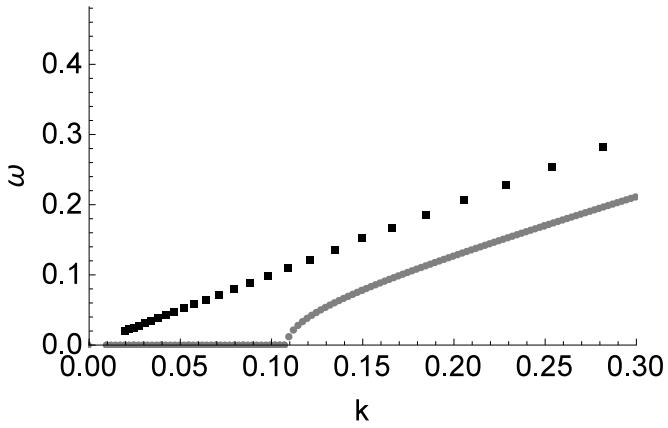

Figure 5.1: Real parts of the dispersion relations with the greatest (least negative, in this case) imaginary part, for $d = 10$, $\psi_0 = 0.3\pi$, $\Delta = -1$. The upper, darker curve corresponds to Neumann boundary conditions and had no imaginary part. The lower, lighter curve, corresponding to Dirichlet boundary conditions, had an imaginary part identical to the circle-curve in Figure 5.3. Note especially the complete linear behaviour for Neumann conditions, and the slight difference in slope between the asymptotes.

5.1.1 d

As argued in [19], one can scale the different fields and parameters with r_T to make the system independent on r_T. Setting $r_T = 1$ thus yields this effect, and $d \to 0$ is the equivalent of no charge and $d \to \infty$ is the equivalent of $T \to 0$, and different balances in between. Increasing d thus decreases the dissipation area of the dispersion relation, and asymptotically the relation gets linear all the way to zero. This is the behaviour expected of a zero sound mode. The result of taking $d \to 0$ is shown in figure 5.2.

5.1.2 ψ_0

Using the intersection angle of the D7-branes as the controlling parameter for the branes does not seem to be the most common way to control the system. A perhaps more common parameter that is equivalent is the m-parameter in the asymptotic expansion. We opted not to use it, as it is implicitly given by ψ_0 and ψ_0 occurs explicitly in the expression. m can also only be identified as a mass if $\Delta = -1$ something we did not want to restrict ourselves to, which severely reduces the intuitive gain of using m. It is also worth mentioning that just as not all values of ψ_∞ are possible with real f_n, not all values of ψ_0 are possible with the desired

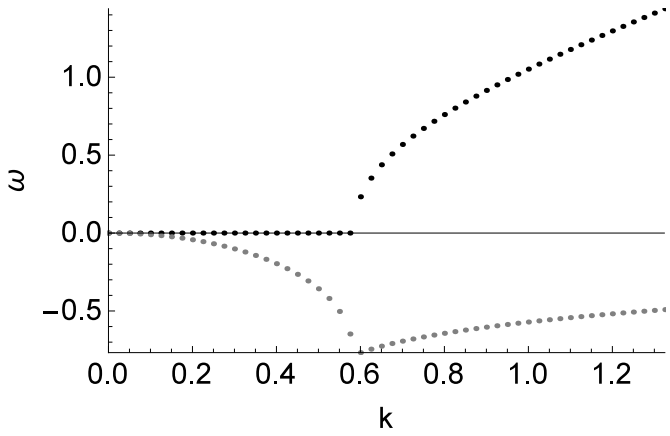

Figure 5.2: Dispersion relation with the greatest (least negative) imaginary part, for $d = 0$, $\psi_0 = 0.3\pi$, $\Delta = -1$ and Dirichlet boundary conditions. The lower curve is the imaginary part and the upper curve is the real part. At $k \approx 0.6$ the displayed mode intersects another mode with a previously lesser (that is, more negative) imaginary part. These two continue as with a positive or negative real part. Here, only the positive real mode is shown.

asymptote of $\psi(r)$. For sufficiently large angles, the solution tends to $\psi_\infty = \pi/2$ (or $\psi_\infty = 0$), which is another trivial solutions, which allows for all possible values of f_n. As two coordinates on the brane disappears for such solutions, we decide to not look further into these "shrinking" embeddings. This sets a constrain of the initial angle to be $0.125\pi < \psi_0 < 0.375\pi$.

When $\psi_0 = \psi_\infty$ the solution is $\psi' = 0$. This decouples several of the differential equations, which significantly helps in the process of identifying what kind of modes are found. Apart from this, the initial angle has a surprisingly small impact. Where one might expect a mass gap such as in [14], none is found. A progression in starting angles, and their corresponding m-values are shown in 5.3.

5.1.3 Δ

The Δ-exponent had, contrary to our hypothesis, a negligible impact on the longitudinal mode. We do expect it to primarily have an effect when m is non-zero although it could possibly have an effect regardless, as f_1 and f_2 are the parameters that decide Δ and these are still present in the equations. A progression in Δ for general parameters are shown in figure 5.4.

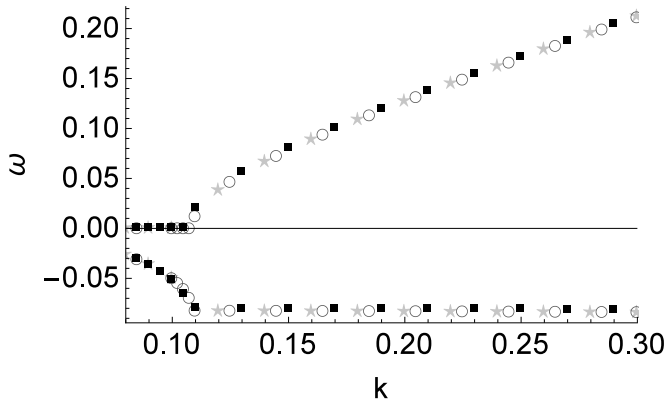

Figure 5.3: Dispersion relation with the greatest (least negative) imaginary part, for $d = 10$, $\Delta = -1$ and Dirichlet boundary conditions. Darker squares, circles and brighter stars correspond to $\psi_0 = 0.35\pi, 0.3\pi, 0.25\pi$ respectively (corresponding to $m = 11.1, 1.46, 0$). The lower points are the imaginary parts and the upper points the real parts. No notable difference between the sets in this particular mode.

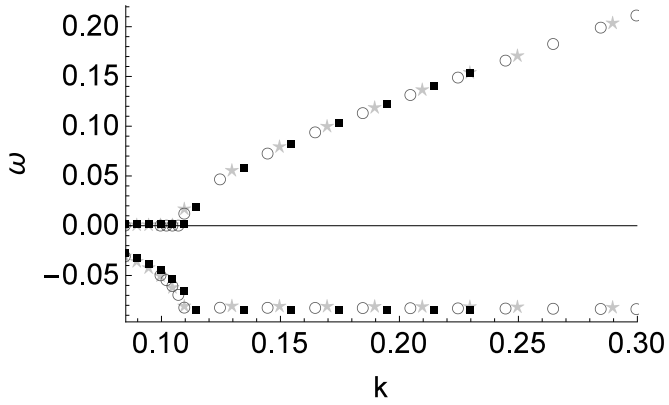

Figure 5.4: Dispersion relation with the greatest (least negative) imaginary part, for $d = 10$, $\psi_0 = 0.3\pi$ and Dirichlet boundary conditions. Darker squares, circles and brighter stars correspond to $\Delta = -1/2, -1, -3/2$ respectively. The lower points are the imaginary parts and the upper points the real parts. No notable difference between the sets in this particular mode.

5.1.4 Boundary conditions

Switching between Dirichlet and Neumann boundary conditions had as expected a relatively large impact. The only mode we could find with Neumann boundary

conditions was perfectly linear $\omega = k$, with no imaginary part. It is an interesting observation, but it is not plasmonic behaviour. A comparison between a general system with either boundary conditions can be seen in figure 5.1. It is worth noting that the real parts, although asymptotically linear, differs slightly in slope. The main difference however is found for small values of k.

Chapter 6

Discussion and Conclusions

6.1 Reliability of the model

The Mathematica inplementation of the model appeared stable. It reproduced the equations of motion from similar articles, as well as the numerical solution to these. It thus seemed that the model was indeed correctly implemented.

6.2 The plasmon mode

We did *not* find the plasmon mode. The implications of this are important enough to warrant a thorough check of the implemented model. The plasmon is a relatively simple phenomenon, compared to other things the model has been used to describe, as for instance the roton in [11]. A model used to describe advanced phenomena that fails to portray the simple ones is not (entirely) reliable. So, where do we fail to describe the plasmon?

6.2.1 Parameter space

It is possible that the plasmon solutions are out there in the model to see, but are simply not located near the values of the parameters we have examined. As our parameter space is relatively large, given the number of parameters we can change, and the ranges for those parameters too, it is possible. It is however unlikely, because we find the zero-sound mode. As described in for instance [14], the zero sound mode turns *into* the plasmon mode when a charge density is added. Regardless of whether we have a charge density or not, the zero sound mode is present, with its very characteristic behaviour of no gap and linear asymptote. It is also a note to be made of the dependence on charge vs dependence on charge carriers. The surface plasmons of [13] scales with the number of charge carriers,

but this is not what we change when we tune d. We rather tune a net charge of the system.

6.2.2 Model improvements

It is possible that this particular behaviour of collective excitation demands that the stack of D7-branes does not yield a negligible contribution to the metric of the system, and thus requires that this is taken into account. This is what is called a "backreaction", and it significantly complicates the model.

It is also possible that the charged fermions needs to be specified more explicitly than in this model. This has been done in "bottom-up" models, where instead of starting from a string theory realisation and adding components, one starts from the gravitational description of stars.

Another less likely prospect is that when we model our system we set the coupling constant to be infinitely strong. This has implications to the curvature length L, which impacts on two particular points. Firstly, for the metric we assume a near horizon theory $r \ll L$, which might seem like a weird thing to keep fixed, even when we let $r \to \infty$. This is done to ensure AdS for all r, and is a very key thing in the duality. Keeping the curvature length relevant in calculations gives another scale parameter, which in this case would impact the temperature radius. We would then have dependencies on the temperature and the charge individually, which in itself seems desirable.

6.3 Outlook

Although it is disheartening that the model did not portray plasmons, this is still an interesting result. The model *should* be able to depict plasmons. Similar models are used to model two-dimensional materials in other contexts, most notably as with some choices of parameters, the conductivities returned are similar to the observed ones. However, if one wants a reliable model of for instance graphene, the model really should be able to reproduce the known behaviours of graphene before one makes daring predictions for graphene based on the results from a model. This result is thus an indicator that these models may be too simple, and needs some further enhancement.

The model in itself still has several more features and areas of applicability that have not been utilized. These include examining other properties and how the system changes when other fields or currents are applied. Once the necessary tweaks to the system have been made, the model can be used to predict these more advanced properties and thus, these have not been explored here.

Bibliography

[1] Ammon, M. and Erdmenger, J. (2015) *Gauge/Gravity Duality.* Cambridge University Press.

[2] Zaanen, J., Sun, Y.W., Liu, Y. and Schalm, K. (2015) *Holographic Duality in Condensed Matter Physics.* Cambridge University Press.

[3] Bergman, O., Jokela, N., Lifschytz, G. and Lippert, M. (2010) *Quantum Hall Effect in a Holographic Model. JHEP*, volume **1010** (063). [arXiv:1003.4965v2 [hep-th]].

[4] Amado, I., Kaminski, M. and Landsteiner, K. (2009) *Hydrodynamics of Holographic Superconductors. JHEP*, volume **0905** (021). [arXiv:0903.2209v3 [hep-th]].

[5] Wallace, P.R. (1947) *The Band Theory of Graphite. Phys. Rev.*, volume **71** (622).

[6] Novoselov et al. (2004) *Electric Field Effect in Atomically Thin Carbon Films. Science*, volume **306** (666). [arXiv:0410550 [cond-mat]].

[7] The Royal Swedish Academy of Sciences. *Scientific Background on the Nobel Prize in Physics 2010: GRAPHENE.* URL `http://www.nobelprize.org/nobel_prizes/physics/laureates/2010/advanced-physicsprize2010.pdf`.

[8] Schulz, H. (1995) *Fermi liquids and non-Fermi liquids.* In *Proceedings of Les Houches Summer School LXI.* Elsevier, Amsterdam. [arXiv:9503150v2 [cond-mat]].

[9] J. Crossno et al. (2016) *Observation of the Dirac fluid and the breakdown of the Wiedemann-Franz law in graphene. Science Magazine*, volume **351** (1058). [arXiv:1509.04713 [cond-mat.mes-hall]].

[10] Maldacena, J.M. (1998) *The large N limit of superconformal field theories and supergravity. Adv. Theor. Math. Phys.*, volume **2**. [arXiv:9711200v3 [hep-th]].

[11] Jokela, N., Lifschytz, G. and Lippert, M. (2011) *Magneto-roton excitation in a holographic quantum Hall fluid. JHEP*, volume **1102** (104). [arXiv:1012.1230v3 [hep-th]].

[12] Stockman, M.I. (2011) *Nanoplasmonics: The physics behind the applications. Physics Today*, volume **62** (2), 39.

[13] Wenger, T. (2015) *Plasmons in Nanostructured Graphene.* Lic. thesis, Chalmers University of Technology.

[14] H. Godfrin et al. (2012) *Observation of a roton collective mode in a two-dimensional Fermi liquid. nature*, volume **483**.

[15] Polchinski, J. (1998) *String Theory Volume II.* Cambridge University Press. pp.153-154.

[16] Myers, R.C. and Wapler, M.C. (2008) *Transport Properties of Holographic Defects. JHEP*, volume **0812** (115). [arXiv:0811.0480v2 [hep-th]].

[17] Omid, H. and Semenoff, G.W. (2013) *D3-D7 holographic dual of a perturbed 3D CFT. Physical Review D*, volume **88**, Iss. 2.

[18] Jokela, N., Lifschytz, G. and Lippert, M. (2013) *Holographic anyonic superfluidity. JHEP*, volume **1310** (014). [arXiv:1307.6336v3 [hep-th]].

[19] Bergman, O., Jokela, N., Lifschytz, G. and Lippert, M. (2011) *Striped instability of a holographic Fermi-like liquid. JHEP*, volume **1110** (034). [arXiv:1106.3883v2 [hep-th]].

[20] Hwang, E. and Sarma, S.D. (2007) *Dielectric function, screening, and plasmons in two-dimensional graphene. Physical Review B*, volume 75.